Synthesis and Catalytic Properties in Olefin Epoxidation of Octahedral Dichloridodioxidomolybdenum(VI) Complexes Bearing N,N-Dialkylamide Ligands: Crystal Structure of [Mo2O4(μ2-O)...

ARTICLE *in* EUROPEAN JOURNAL OF INORGANIC CHEMISTRY · OCTOBER 2009

Impact Factor: 2.94 · DOI: 10.1002/ejic.200900544

DOI: 10.1002/ejic.200900544

Synthesis and Catalytic Properties in Olefin Epoxidation of Octahedral Dichloridodioxidomolybdenum(VI) Complexes Bearing *N*,*N*-Dialkylamide Ligands: Crystal Structure of $[Mo_2O_4(\mu_2\text{-}O)Cl_2(dmf)_4]$

Sandra Gago,[a] Patrícia Neves,[a] Bernardo Monteiro,[a] Márcia Pessêgo,[b] André D. Lopes,[b] Anabela A. Valente,[a] Filipe A. Almeida Paz,[a] Martyn Pillinger,[a] José Moreira,[b] Carlos M. Silva,[a] and Isabel S. Gonçalves*[a]

Keywords: Molybdenum / O ligands / Homogeneous catalysis / Epoxidation / Kinetics

The catalytic performance of the complexes $[MoO_2Cl_2(L)_2]$ [L = *N*,*N*-dimethylformamide (dmf), *N*,*N*-dimethylacetamide (dma), *N*,*N*-dimethylpropionamide (dmpa), *N*,*N*-diethylformamide (def) and *N*,*N*-diphenylformamide (dpf)] was examined in the epoxidation of *cis*-cyclooctene with *tert*-butyl hydroperoxide (tbhp) at 55 °C and in the absence of a cosolvent. The complexes showed high turnover frequencies in the range of 561–577 $mol\,mol_{Mo}^{-1}\,h^{-1}$, giving the epoxide as the only product in ≥98 % yield after 6 h. The reaction rates decreased significantly in consecutive runs carried out by recharging the reactors with olefin and oxidant. On the basis of the IR spectroscopic characterisation of the solids recovered at the end of the catalytic reactions, the decrease in activity is attributed to the formation of dioxido(μ-oxido)-molybdenum(VI) dimers. Accordingly, the treatment of $[MoO_2Cl_2(dmf)_2]$ with an excess amount of tbhp led to the isolation of $[Mo_2O_4(\mu_2\text{-}O)Cl_2(dmf)_4]$, which was characterised by single-crystal X-ray diffraction and found to exhibit a catalytic performance very similar to that found in the second runs for the mononuclear complexes. The kinetics of the reaction of $[MoO_2Cl_2(dmf)_2]$ with tbhp was further examined by UV/Vis spectroscopy, allowing rate constants and activation parameters to be determined. For the dpf adduct, the effect of different solvents on cyclooctene epoxidation and the epoxidation of other olefins, namely, (*R*)-(+)-limonene, α-pinene and norbornene, were investigated.

Introduction

Dioxidomolybdenum(VI) complexes of the type $[MoO_2X_2(L)_n]$ are of interest as models for molybdoenzymes,[1] as oxo-transfer agents[2] and as (pre)catalysts for the liquid-phase epoxidation of olefins.[3] A broad range of complexes have been studied with different anionic X (F, Cl, Br, alkyl, OR, $OSiR_3$, SR) and neutral L ligands. The L ligands may involve either two monodentate ligands (e.g., dmf,[2c,4] thf,[5] R_2SO,[1d,2,6] RCN,[7] H_2O,[2c,8] OPR_3[1e,2c,3e–3g,9]) or one bidentate ligand containing oxygen,[3f,10] nitrogen[1d,3a–3d,11] or sulfur[12] donor atoms. With a few exceptions, all of these complexes adopt a *cis*-oxido, *trans*-X, *cis*-L configuration at the metal centre and a distorted octahedral coordination geometry.[13] Adducts of MoO_2X_2 (X = Cl, Br) with the solvent molecules dmf, thf, R_2SO and RCN have been investigated in several catalysed reactions, such as the oxidation of triphenylphosphane to triphenylphosphane oxide with dimethyl sulfoxide (dmso),[2] the oxidation of thiols to disulfides with dmso,[2b,2c,14] the aerobic oxidation of activated benzyl alcohols to the corresponding aldehydes,[15] the epoxidation of olefins[7,16] and the reductive cyclisation of nitrobiphenyls and nitrostyrenes to carbazoles and indoles.[17] The epoxidation of cyclooctene with *tert*-butyl hydroperoxide (tbhp) in the presence of $[MoO_2Br_2(RCN)_2]$ (R = CH_3 or C_6H_5) quickly reached a conversion of about 65% but did not proceed significantly further.[7] This was attributed to the pronounced water sensitivity of the complex. In contrast, the complex $[MoO_2Cl_2(dmf)_2]$ displayed a much higher catalytic activity (95% cyclooctene epoxide after 2 h at 55 °C; 100% after 24 h).[16b] The catalytic stability of this system was investigated by recharging the reaction vessel with substrate and oxidant after 24 h. Initially, the reaction was somewhat slower in the second run, but after 1 h the kinetic curves for the two runs converged to give the same conversion of about 98% after 6 h. We have now extended this study to cover four other *N*,*N*-disubstituted amides in order to investigate the electronic and steric effects of the substituents (H, methyl, ethyl, phenyl) on the carbonyl group and nitrogen atom on the catalytic performance of the resultant

[a] Department of Chemistry, CICECO, University of Aveiro, 3810-193 Aveiro, Portugal
E-mail: igoncalves@ua.pt
[b] Faculty of Science and Technology, Department of Chemistry, Biochemistry and Pharmacy, University of the Algarve, Campus de Gambelas, 8005-136 Faro, Portugal
Supporting information for this article is available on the WWW under http://dx.doi.org/10.1002/ejic.200900544.

$[MoO_2Cl_2(RCONR'_2)_2]$ complexes. With the aim of obtaining a better understanding of the catalytically active species formed under the reactions conditions used, the reaction of the complexes with tbhp was examined in more detail by (1) isolating and characterising the product formed upon treatment of $[MoO_2Cl_2(dmf)_2]$ with an excess amount of the oxidant in dmf and (2) using UV/Vis spectroscopy to follow the kinetics, allowing rate constants and activation parameters to be determined.

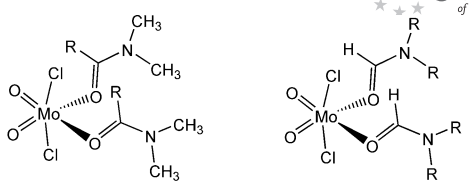

R = H (**1**), CH_3 (**2**), CH_3CH_2 (**3**) R = CH_3CH_2 (**4**), Ph (**5**)

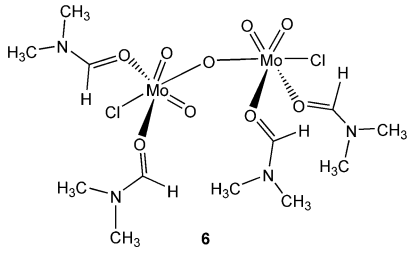

6

Results and Discussion

Synthesis and Characterisation of the Dioxidomolybdenum(VI) Complexes

Bis(*N*,*N*-dimethylformamide)dichloridodioxidomolybdenum(VI) (**1**) was synthesised as described previously by treatment of an aqueous hydrochloric acid solution of MoO_3 with an excess amount of dmf.[8a] For the other amides, the direct reaction of MoO_2Cl_2 with two equivalents of the ligand in CH_2Cl_2 solution gave adducts **2**–**5** in good yields as pale-yellow powders, soluble in CH_2Cl_2, and insoluble in diethyl ether, hexane and pentane. In contrast to the acetonitrile and thf adducts, both of which are air and moisture sensitive and can only be handled and stored under dry inert gas atmosphere, compounds **1**–**5** are air stable. The IR and Raman spectra contain a pair of bands in the ranges 940–950 and 905–915 cm^{-1}, which are assigned to the symmetric and asymmetric stretching vibrations of the *cis*-$[MoO_2]^{2+}$ group, respectively. The corresponding frequencies for the acetonitrile and thf adducts lie at higher values (ca. 960 and 920 cm^{-1}), consistent with the stronger coordination of the amide ligands in **1**–**5**.[18] The IR spectra of all five compounds afford conclusive evidence that the amide is coordinated through the oxygen atom. Thus, the carbonyl stretching frequency, which occurs at 1640–1670 cm^{-1} in the free ligands, is lowered by 20–50 cm^{-1} to 1602–1653 cm^{-1} in the complexes. This result is explained by the decrease in the double-bond character of C=O and the subsequent increase in the C–N double bond character.[19] The relatively large range of shifts in ν(C=O) upon complexation (which could be interpreted to mean Mo^{VI}–carbonyl interactions of varying strengths) are not paralleled by the stretching frequencies for the *cis*-$[MoO_2]^{2+}$ group, which all fall within relatively narrow ranges.

Treatment of $[MoO_2Cl_2(dmf)_2]$ with a large excess of tbhp (15 equiv.) in decane/dmf led to the isolation of the μ-oxido binuclear molybdenum(VI) complex $[Mo_2O_4(\mu_2\text{-}O)Cl_2(dmf)_4]$ (**6**). The IR spectrum of **6** supports the presence of the *cis*-$[MoO_2]^{2+}$ group ($\nu_{Mo=O}$ = 903 and 948 cm^{-1}), the Mo–O–Mo linkage ($\nu_{Mo-O-Mo}$ = 767 cm^{-1}) and dmf ligands coordinated through oxygen (ν_{CO} = 1649 cm^{-1}). Even though the ambient temperature crystallographic description of this material was reported by Atovmyan et al. in 1970,[20] the 3D coordinates are not deposited in the most recent version of the Cambridge Structural Database (CSD, Version 5.30, November 2008 with 1 update).[21] Furthermore, the indicative *R* factor was quite high (>10%), and the original paper does not contain the fractional atomic coordinates. For these reasons, the structure of **6** was redetermined by single-crystal X-ray diffraction at the low temperature of 100(2) K by using a significantly better resolution of up to 0.70 Å. Since the paper by Atovmyan et al.,[20] only three other structures of binuclear oxido-bridged Mo^{VI} complexes bearing dmf ligands have been reported, namely, $[Mo_2O_5(hpb)_2(dmf)_4]$ (hpb = 2-*o*-hydroxyphenylbenzimidazole) by Caparelli et al.[22] and $[Mo_2O_3(3\text{-}t\text{-}Bussp)_2(dmf)_2]$ and $[Mo_2O_3(3\text{-}EtOssp)_2(dmf)_2]\cdot 2dmf$ by Holm and coworkers (3-*t*-Bussp = 3-*tert*-butylsalicylaldehyde; 3-EtOssp = 3-ethylsalicylaldehyde).[23]

The binuclear $[Mo_2O_5Cl_2(dmf)_4]$ molecular unit in **6** has crystallographic C_2 symmetry around the central μ_2-bridging oxido group (Figure 1), which imposes a Mo(1)···Mo(1)^i distance of 3.783(1) Å and subtends a Mo(1)–(μ_2-O)–Mo(1)^i angle of 175.02(15)° [symmetry code: (i) 1 – *x*, *y*, 1.5 – *z*]. The crystallographically unique Mo^{VI} centre is coordinated by two dmf molecules, one chlorido ligand, two terminal oxido groups and the central μ_2-bridging oxido moiety, with the overall {$MoClO_5$} coordination geometry resembling a highly distorted octahedron. Whereas the Mo–(O,Cl) bond lengths fall in the range 1.6983(19)–2.4394(6) Å, the internal *cis* and *trans* octahedral angles are in the ranges 78.08(7)–103.46(9)° and 159.47(4)–167.87(8)°, respectively (Figure 1 and Table 1). The wide ranges in these geometrical values arise from the different chemical nature of each ligand composing the first coordination sphere. Indeed, the Mo=O bonds clearly exert the typical *trans* effect by displacing the Mo^{VI} centre from the O(1)→Cl(1) vector by about 0.35 Å, with the former bonds being the shortest registered for the binuclear complex [1.6984(18) and 1.6983(19) Å], contrasting well with those to the *trans*-oxido-coordinated dmf molecules [Mo–O bond lengths of 2.2581(18) and 2.2321(17) Å], also composing the equatorial plane of the octahedron. The two symmetry-related chlorido ligands are located in the apical positions, thereby minimising overall steric repulsion. The Mo=O and Mo–Cl bond lengths (Table 1) are typical of oxidomolybde-

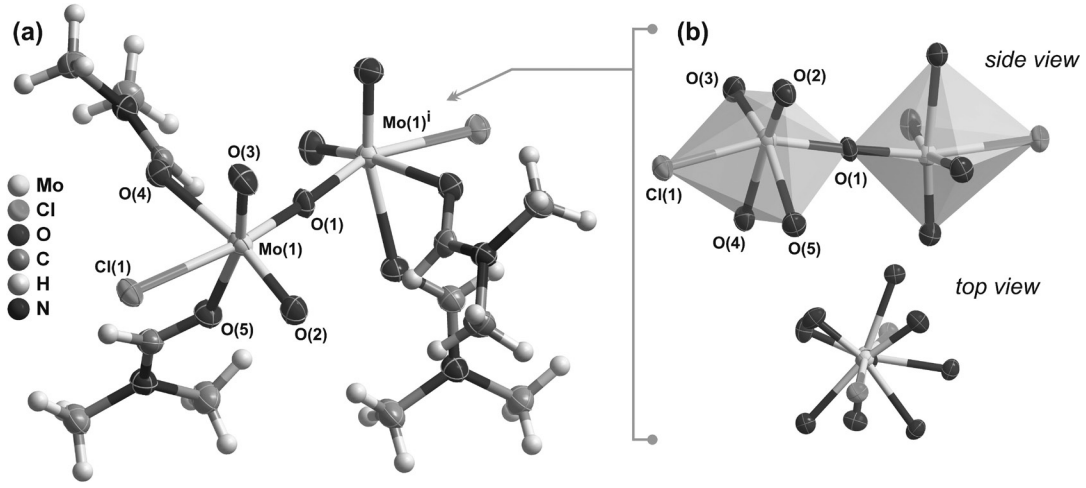

Figure 1. (a) Schematic representation of $[Mo_2O_4(\mu_2\text{-}O)Cl_2(dmf)_4]$ (**6**) with all non-hydrogen atoms being represented as thermal ellipsoids drawn at the 70% probability level, hydrogen atoms as small spheres with arbitrary radii, and showing the labelling scheme for the atoms composing the first coordination sphere of Mo(1). (b) Top and side views of the $\{Mo_2Cl_2O_9\}$ core. For selected bond lengths and angles see Table 1. Symmetry transformation used to generate equivalent atoms: (i) $1 - x$, y, $1.5 - z$.

num complexes, as revealed by systematic searches in the CSD [$d_{Mo=O}$ = 1.60–2.51 Å (1246 entries, median of ca. 1.71 Å); d_{Mo-Cl} = 2.17–2.74 Å (67 entries, median of ca. 2.37 Å)]. Interestingly, the Mo–O bonds with dmf are remarkably shorter than those reported for related dioxidomolybdenum complexes with this ligand [values found in the range 2.31–2.70 Å].[4b,23–25] This difference is explained by the fact that the crystallographic data used here were collected at the low temperature of 100(2) K, whereas the data used in the cited references were all collected at ambient temperature.

Table 1. Selected bond lengths [Å] and angles [°] for the Mo^{VI} coordination environment present in complex $[Mo_2O_4(\mu_2\text{-}O)Cl_2(dmf)_4]$ (**6**).[a]

Mo(1)–O(1)	1.8934(3)	Mo(1)–O(4)	2.2581(18)
Mo(1)–O(2)	1.6984(18)	Mo(1)–O(5)	2.2321(17)
Mo(1)–O(3)	1.6983(19)	Mo(1)–Cl(1)	2.4394(6)
O(1)–Mo(1)–O(4)	82.69(5)	O(3)–Mo(1)–O(2)	103.46(9)
O(1)–Mo(1)–O(5)	82.87(8)	O(3)–Mo(1)–O(4)	87.77(8)
O(1)–Mo(1)–Cl(1)	159.47(4)	O(3)–Mo(1)–O(5)	164.70(8)
O(2)–Mo(1)–O(1)	99.30(7)	O(3)–Mo(1)–Cl(1)	90.04(6)
O(2)–Mo(1)–O(4)	167.87(8)	O(4)–Mo(1)–Cl(1)	80.64(5)
O(2)–Mo(1)–O(5)	90.26(8)	O(5)–Mo(1)–O(4)	78.08(7)
O(2)–Mo(1)–Cl(1)	94.61(6)	O(5)–Mo(1)–Cl(1)	82.04(5)
O(3)–Mo(1)–O(1)	101.22(9)	$Mo(1)^i$–O(1)–Mo(1)	175.02(15)

[a] Symmetry transformation used to generate equivalent atoms: (i) $1 - x$, y, $1.5 - z$.

Individual $[Mo_2O_4(\mu_2\text{-}O)Cl_2(dmf)_4]$ complexes close pack in the solid state with the self-assembly being driven mainly by the need to effectively fill the space while mediated by a few rather weak C–H···(O,Cl) interactions (not shown). Undulated layers placed in the *ac* plane of the unit cell and composed of binuclear complexes pack in a parallel fashion along the direction of the *b* axis (Figure 2) to give the crystal structure of **6**.

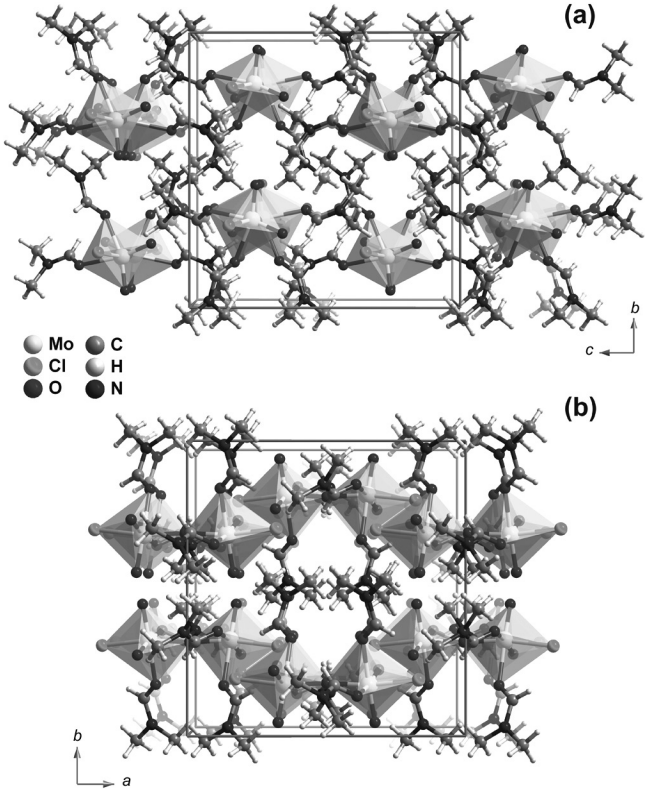

Figure 2. Perspective views of the crystal packing along the (a) [100] and (b) [001] crystallographic directions in the structure of $[Mo_2O_4(\mu_2\text{-}O)Cl_2(dmf)_4]$ (**6**). Mo^{VI} metal centres are represented as distorted $\{MoClO_5\}$ octahedra.

Catalytic Tests

Complexes **1**–**5** are active catalysts for the epoxidation of *cis*-cyclooctene at 55 °C, using tbhp (5.5 M in decane) as the oxidant without a cosolvent, and give 1,2-epoxycyclooctane

as the only product. The noncatalytic contribution is negligible. The kinetic profiles are nearly coincident (Figure 3) and the observed initial TOF values lie in the narrow range of 561–577 mol mol$_{Mo}^{-1}$ h^{-1} (Table 2). These are the first indications that the active species and reaction mechanism may be similar for all five complexes. Initially, cyclooctene conversion increased abruptly reaching at least 92% at 10 min and 98–99% after 6 h. The sudden slowdown of the reaction with time is typical of dioxidomolybdenum(VI) complexes of the type [$MoO_2X_2(L)_n$] [where $(L)_n$ is one bidentate or two monodentate Lewis base N,O ligands] used as catalysts in the same reaction, under similar conditions.[3a,26,27] One explanation for this behaviour is that the accumulation of *tert*-butyl alcohol, formed as a byproduct of the decomposition of tbhp, during the batch-wise reaction is detrimental because it is able to coordinate to the metal centre, blocking free coordination sites for the activation of the olefin. On the other hand, transformations of the active species into less-active ones, such as oxidising species with lower electrophilicity at the peroxido functionality, cannot be ruled out.

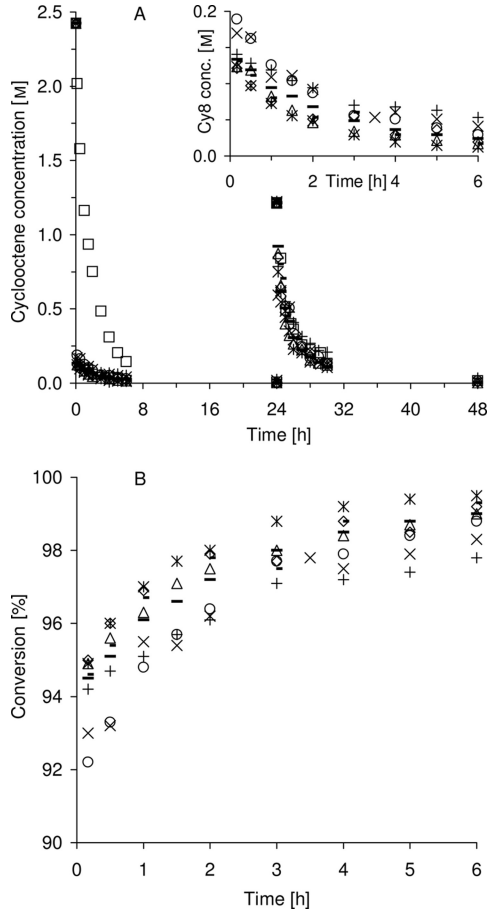

Figure 3. (A) Cyclooctene concentration as a function of reaction time in two consecutive 24 h runs at 55 °C by using tbhp (5.5 M in decane) without a cosolvent, in the presence of **1** (×), **2** (○), **3** (△), **4** (+), **5** (-), **6** (□), MoO_2Cl_2 (∗), [$MoO_2Cl_2(thf)_2$] (◇) and [$MoO_2Cl_2(CH_3CN)_2$] (–). The inset shows in detail the behaviour during the first 6 h of the first run for all complexes except [$Mo_2O_4(\mu_2\text{-}O)Cl_2(dmf)_4$] (**6**). (B) Cyclooctene conversion as a function of time (in the first run) for all complexes except **6**.

Table 2. *cis*-Cyclooctene epoxidation with tbhp (in decane) at 55 °C in the presence of the Mo complexes.

Molybdenum complex	TOF[a] [mol mol$_{Mo}^{-1}$ h^{-1}]	Conversion[b] [%] Run 1	Run 2
1	565	98/99	90/99
2	561	99/100	90/99
3	577	99/100	91/100
4	574	98/99	83/97
5	575	99/100	91/100
6	102	94/100	89/99
[$MoO_2Cl_2(thf)_2$]	573	99/100	89/100
[$MoO_2Cl_2(CH_3CN)_2$]	571	99/100	91/100

[a] Turnover frequency calculated at ca. 10 min. [b] Cyclooctene conversion calculated at 6/24 h for runs 1 and 2. The epoxide selectivity was always 100%.

The influence of the solvent on cyclooctene epoxidation in the presence of diphenylformamide adduct **5** was investigated at 55 °C (Table 3, Figure 4). Depending on whether the solvent was ethanol, acetonitrile or 1,2-dichloroethane (dce), the catalytic activity changed considerably without affecting epoxide selectivity, which was always 100%. Although the complex is more soluble in CH_3CN or ethanol (transparent solutions were obtained) than in dce (the mixture was opaque, as observed without cosolvent), the reaction was faster in the latter case, leading to more than 99% conversion after 10 min, which is somewhat higher than that observed when no cosolvent was used. The negative effect of CH_3CN and especially of ethanol on initial catalytic activity may be due to the coordinating abilities of these solvent molecules, consistent with the above discussion concerning the negative effect of the byproduct *tert*-butyl alcohol on the overall reaction rate. It is also possible that metal–ligand dissociation (discussed below) is enhanced in the presence of these coordinating solvents, originating less-active species.

Table 3. Olefin epoxidation at 55 °C with the use of complex **5**, tbhp (in decane) and different cosolvents.

Olefin	Cosolvent	TOF[a] [mol mol$_{Mo}^{-1}$ h^{-1}]	Conv.[b] [%]	Select.[b] [%]
Cyclooctene	none	575	99/100	100/100
Cyclooctene	ethanol	91	86/99	100/100
Cyclooctene	CH_3CN	516	89/91	100/100
Cyclooctene	dce	605	100/100	100/100
(*R*)-(+)-Limonene	dce	205	92/98	90/73[c]
α-(+)-Pinene	dce	52	21/28	<1[d]
Norbornene	dce	321	96/100	92/81[e]

[a] Turnover frequency calculated at ca. 10 min. [b] Olefin conversion and epoxide selectivity calculated at 6/24 h. [c] Sum of selectivities to 1,2-epoxy-*p*-menth-8-ene and 1,2–8,9-diepoxy-*p*-menthane. At 24 h, the epoxide/diepoxide mol ratio was 0.7. [d] Selectivity to campholenic aldehyde at 6/24 h was 61/51%. Epoxy campholenic aldehyde and small amounts of other unidentified products were formed. [e] Dihydroxybicyclo[2,2,1]heptane and small amounts of other unidentified products were formed.

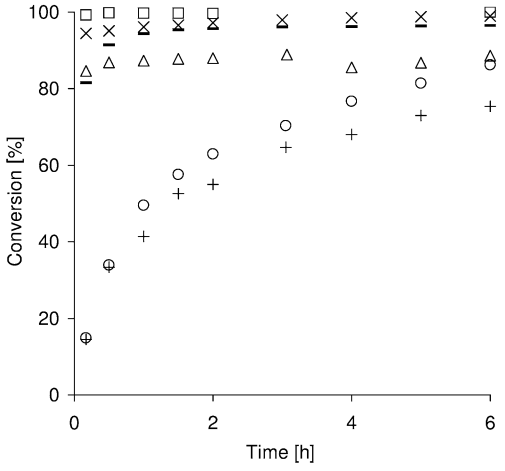

Figure 4. Kinetic profiles of cyclooctene epoxidation in the presence of **5** by using tbhp (5.5 M in decane) without a cosolvent at 55 °C (×) or 30 °C (-) or by using 1,2-dichloroethane (□), ethanol (○) or acetonitrile (△) as cosolvents at 55 °C, or using aqueous tbhp (70 wt.-%) without a cosolvent at 55 °C (+).

The epoxidation of other olefins, namely, (*R*)-(+)-limonene, α-pinene and norbornene, was investigated for **5** with the use of dce as cosolvent, at 55 °C (Table 3). The reaction of limonene gave 1,2-epoxy-*p*-menth-8-ene and 1,2–8,9-diepoxy-*p*-menthane as the main products and the respective diols as byproducts; after 24 h the total epoxide yield was 72% against 26% of diols (small amounts of other unidentified products were also formed). The reaction of α-pinene was much slower and gave mainly campholenic aldehyde (until 28% conversion), an important intermediate used in the fragrance industry for the synthesis of santalol, which is the principle component of sandalwood oil.[28,29] The amount of α-pinene oxide detected was residual (<1% yield), possibly because it undergoes Lewis acid catalysed isomerisation to give campholenic aldehyde (13% yield after 6 h).[28,29] Norbornene was reactive with tbhp in the absence of a catalyst, giving epoxynorbornane as the only product. Although the initial reaction rate was relatively slow, 63% conversion was achieved after 24 h. In the presence of **5**, the TOF was much higher (321 $mol\,mol_{Mo}^{-1}\,h^{-1}$) than without catalyst, and selectivity to epoxynorbornane was 96% at 62% conversion, decreasing to 81% at 100% conversion.

When the temperature of the cyclooctene reaction in the presence of **5** was lowered from 55 to 30 °C, the initial TOF decreased from 575 to 496 $mol\,mol_{Mo}^{-1}\,h^{-1}$, without affecting epoxide selectivity. However, after 1 h, approximately the same conversion was reached (94–97%, Figure 4). The use of 70 wt.-% aqueous tbhp instead of the 5.5 M decane solution gave a liquid–liquid biphasic system, and the reaction rate at 55 °C decreased significantly (TOF decreased from 575 to 88 $mol\,mol_{Mo}^{-1}\,h^{-1}$, Figure 4). The following factors may contribute to the lower catalytic activity: (1) Mass transfer limitations and the distribution of tbhp in the liquid–liquid biphasic system. (2) The coordinating ability of the water molecules (inhibitory effect). (3) Partial catalyst deactivation through, for example, hydrolysis. Nevertheless, after 24 h, cyclooctene conversion reached 93% and epoxide selectivity was 100%.

The catalyst stability was investigated for **1**–**5** by carrying out two consecutive runs of cyclooctene epoxidation at 55 °C by using tbhp (in decane) without cosolvent. After the first run of 24 h, the reactor was recharged with olefin and oxidant in equivalent amounts to those used in the first run. As found for the first runs, the kinetic curves for the second runs were practically coincident for all five systems (Figure 3), and epoxide selectivity was always 100%. Although the initial reaction rate decreased from the first to the second run, the epoxide yield after 24 h was practically the same for both runs (>97%). These results are far superior to the reported behaviour of $[MoO_2Br_2(CH_3CN)_2]$, which was completely deactivated after approximately 2 h, giving a maximum conversion of 65%.[7] For comparison, two consecutive runs of cyclooctene epoxidation were carried out by using MoO_2Cl_2, $[MoO_2Cl_2(thf)_2]$ and $[MoO_2Cl_2(CH_3CN)_2]$ as (pre)catalysts, under similar conditions to those used for **1**–**5**. Upon exposure to air, the initially pale-yellow MoO_2Cl_2 rapidly turned blue, which is indicative of Mo^V species. However, the yellow colour was restored in the presence of tbhp. The catalytic performance of the three systems was very similar to that for **1**–**5**, giving a TOF in the range of 571–576 $mol\,mol_{Mo}^{-1}\,h^{-1}$ for the first run, and practically coincident kinetic profiles for both runs (Figure 3, Table 2). This implies that the coordinated solvent molecules in the starting complexes of the type $[MoO_2Cl_2(L)_2]$ do not have a significant influence on the outcome of the catalytic olefin epoxidation. Possibly, the steric and electronic (supported by the FTIR data discussed above) effects on the activity of the complexes are similar (activation parameters obtained by UV/Vis are similar, as discussed below) for the distinct monodentate, labile ligands (which may explain the similar initial TOFs for the fresh catalysts) and/or the latter become at least partially dissociated under the reaction conditions used, originating active species that are somewhat alike in the second run.

As described above, treatment of $[MoO_2Cl_2(dmf)_2]$ (**1**) with a large excess of tbhp (15 equiv.) in decane/dmf led to the isolation of the μ-oxido binuclear molybdenum(VI) complex $[Mo_2O_4(\mu_2\text{-}O)Cl_2(dmf)_4]$ (**6**). This complex was tested in two consecutive runs of catalytic *cis*-cyclooctene epoxidation at 55 °C, under similar conditions to those used for **1**–**5**. The epoxide was the only observed product. The profiles for **6** in runs 1 and 2 were very similar (Figure 3). Whereas in the first run the reaction was slower for **6** (TOF = 102 $mol\,mol_{Mo}^{-1}\,h^{-1}$) than for **1**–**5** (TOF = 565–577 $mol\,mol_{Mo}^{-1}\,h^{-1}$), in the second run the kinetic profiles were essentially coincident for **1**–**6**. This suggests that the formation of μ-oxido binuclear molybdenum(VI) species from starting complexes **1**–**5** is likely to play an important role with respect to the main species responsible for the catalytic reactions in the second runs.

The reaction systems formed using complexes **1**–**6** and MoO_2Cl_2 are not homogeneous when no solvent is added. After catalytic runs of 24 h for cyclooctene epoxidation at

55 °C, the solids were separated by centrifugation, washed thoroughly with hexane, dried at room temperature (giving ca. 10 wt.-% of the amounts of complexes initially charged to the reactor) and characterised by FTIR spectroscopy. The spectra in the region 500–1000 cm^{-1} were very similar for all recovered materials, showing six medium-strong non-ligand absorptions at 555–570, 620–630, 685–700, 778–798, 882–902 and 950–960 cm^{-1}, which resemble the six nonligand bands exhibited by complex **6** at 567, 630, 681, 767, 903 and 948 cm^{-1}. In contrast, the amide ligand absorptions in the region 1000–1700 cm^{-1} were either absent or reduced to very weak intensity (compared with complexes **1**–**6**) for the recovered solids. This was backed up by elemental analysis of the solid recovered after catalysis using dmf adduct **1**, which revealed a significant reduction in the amount of C (from 8.0 to 2.7 wt.-%), N (from 20.5 to 8.9 wt.-%) and H (from 4.3 to 2.5 wt.-%). For complex **5**, GC–MS analysis of the reaction solution showed the presence of free *N*,*N*-diphenylformamide.

For complex **5**, the solid (denoted **5**-S) and liquid (denoted **5**-L) phases were separated after a first run by centrifugation and filtration using a 0.2 μm PVDF w/GMF Whatman membrane. After washing with *n*-hexane and drying at room temperature, colourless **5**-S was tested in a second run by adding oxidant and olefin in amounts proportional to those used in the first run. The reaction of cyclooctene in the presence of **5**-S gave 55%/95% conversion at 30 min/6 h, indicating that the solid is active albeit the reaction rate is lower than that observed for **5** (95%/99% conversion at 30 min/6 h). The activity of the homogeneous phase was investigated by recharging oxidant and olefin (in the same amounts as those used in the first run for **5**) to the **5**-L solution and monitoring the reaction for a further 6 h, during which time no solid precipitated. The recycled **5**-L gave 51%/85% conversion after 1 h/6 h, which is comparable with that observed for the second run of **5** without separating the solid (58%/91% after 1 h/6 h, Figure 3A). Hence, the catalytic reaction is essentially homogeneous, albeit a minor amount of active solid is present in the first run.

Taken together with the catalytic performances described above, it seems that (1) the nature of the active species formed under the reaction conditions used is similar for all the investigated complexes, (2) (in)soluble active species possessing the $[(MoO_2)_2(\mu\text{-}O)]^{2+}$ core are formed during the first run, (3) the catalytic reaction is mainly due to active species in homogeneous phase and (4) the solid fraction contains active species formed upon metal–ligand dissociation.

UV/Vis Kinetic Studies of the Reaction of 1–5 with tbhp

The reaction of $[MoO_2Cl_2(L)_2]$ (**1**–**5**) with tbhp at 20–50 °C was followed by UV/Vis spectroscopy (in acetonitrile). Control experiments carried out in the absence of tbhp showed no spectral changes with time. Under the conditions described in the Experimental Section, with tbhp present in a large excess over the catalyst precursor, the reactions follow reversible pseudo-first-order kinetics. A typical set of spectra are given in the Supporting Information for the reaction of $[MoO_2Cl_2(dmf)_2]$ (**1**) (4×10^{-4} mol dm^{-3}) with tbhp (0.03 mol dm^{-3}) at 25 °C. Over 4 h an absorbance at 300 nm decreased with time and an absorbance in the range 323–400 nm increased (due to the formation of a new species) generating an isosbestic point at 323 nm. The absorbance–time curves fit to a first-order exponential equation, $A_t = (A_0 - A_\infty)\exp(-k_{obs}t) + A_\infty$, where A_t, A_0 and A_∞ are the absorbance values at time t, at $t = 0$ and at equilibrium, respectively, and k_{obs} is the observed rate constant. Figure 5 shows a typical fit to absorbance (λ = 300 nm) versus time data for the reaction of $[MoO_2Cl_2(dmpa)_2]$ (**3**) with tbhp at 25 °C; all k_{obs} values are given in the Supporting Information. The fit of k_{obs} values against oxygen donor concentration shows a clear first-order dependence on [tbhp], as exemplified in Figure 6 for $[MoO_2Cl_2(dma)_2]$ (**2**) at 25 °C,

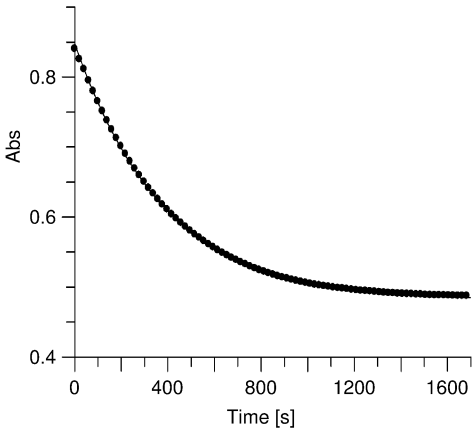

Figure 5. Absorbance (λ = 300 nm) against time data for the reaction of $[MoO_2Cl_2(dmpa)_2]$ (**3**) with tbhp (the solid line shows the fit to a first order decay equation). Reaction conditions: concentration of complex **3** = 4.0×10^{-4} mol dm^{-3}, [tbhp] = 3.0×10^{-2} mol dm^{-3}, solvent = CH_3CN with less than 1% of decane, T = 25 °C.

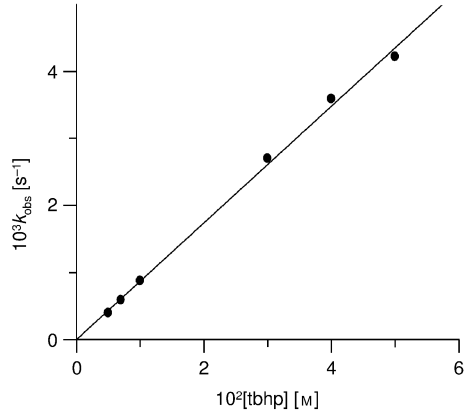

Figure 6. Reversible pseudo-first-order observed rate constants, k_{obs}, at different [tbhp] values. Reaction conditions: concentration of $[MoO_2Cl_2(dma)_2]$ (**2**) = 3.0×10^{-4} mol dm^{-3}, solvent = CH_3CN with less than 1% of decane, T = 25 °C.

and the slope gives the apparent second-order rate constant (k) for the reaction of the Mo complex with tbhp. The k values increased significantly with temperature (Table 4).

Table 4. Measured second-order rate constants, k, at different temperatures for the reaction of complexes **1**–**5** with tbhp.[a]

T [°C]	Complex **1**	Complex **2**	Complex **3**	Complex **4**	Complex **5**
20	5.0 ± 0.2	4.87 ± 0.07	3.1 ± 0.1	4.2 ± 0.2	5.0 ± 0.2
25	7.1 ± 0.4	8.7 ± 0.2	5.6 ± 0.4	7.3 ± 0.3	7.7 ± 0.3
35	19.7 ± 0.8	25 ± 1	18 ± 1	18.7 ± 0.4	21 ± 1
40	32 ± 2	34 ± 2	28 ± 2	28 ± 1	36 ± 1
50	70 ± 3	67 ± 4	51 ± 1	58 ± 3	65 ± 2

[a] Values are $10^2 k$ [$mol^{-1}\,dm^3\,s^{-1}$].

Following the Eyring equation (for an ideal system), plots of $\ln(kh/k_BT)$ versus $1/T$, where h is Planck's constant and k_B is the Boltzmann constant, gave straight lines with slope $-\Delta H^{\neq}/R$ and intercept $\Delta S^{\neq}/R$ (Figure 7). The activation parameters are collected in Table 5. The k values at a given temperature and the $\Delta H^{\neq}$ values are similar for all five complexes, which parallels the similar initial activity observed for all five complexes in the epoxidation of cyclooctene with tbhp. Furthermore, the values of the activation parameters are of the same order of magnitude as those determined previously (using the same method) for complexes of the type $[MoO_2Cl_2L]$, where L is a bidentate Lewis base ligand.[26] The negative $\Delta S^{\neq}$ values were interpreted to support an associative mechanism involving the formation of one adduct between the oxygen donor, tbhp and the metal centre. It is also possible that solvation of the reagents and intermediate species leads to increased ordering in the surrounding solvent. For the catalytic systems studied in the present work, we assume that the active intermediate is mainly responsible for the very high initial olefin epoxidation rates in the first runs. One hypothesis for the catalytic behaviour at longer reaction times and in the second runs is that the intermediate rapidly reacts with tbhp and/or residual water to give an oxido-bridged bimetallic species, which may further react with tbhp to give a second type of active intermediate that is increasingly responsible for the epoxidation reaction. The kinetic studies suggest that the reaction of the precursor with tbhp is a primary rate-determining elementary step.

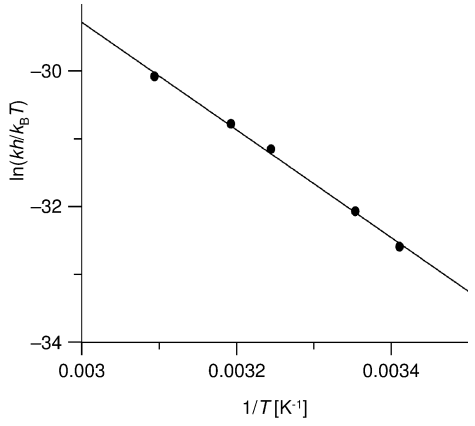

Figure 7. Fit of the second-order rate constants, k, to the Eyring equation (T = 20–50 °C) for complex $[MoO_2Cl_2(def)_2]$ (**4**; def = *N*,*N*-diethylformamide).

Table 5. Values of activation parameters obtained for the different molybdenum complexes.

Complex	$\Delta H^{\neq}$ [$kJ\,mol^{-1}$]	$\Delta S^{\neq}$ [$J\,mol^{-1}\,K^{-1}$]
$[MoO_2Cl_2(dmf)_2]$ (**1**)	68 ± 2	–38 ± 7
$[MoO_2Cl_2(dma)_2]$ (**2**)	67 ± 4	–42 ± 14
$[MoO_2Cl_2(dmpa)_2]$ (**3**)	73 ± 6	–23 ± 18
$[MoO_2Cl_2(def)_2]$ (**4**)	66 ± 2	–45 ± 7
$[MoO_2Cl_2(dpf)_2]$ (**5**)	67 ± 3	–40 ± 11

Concluding Remarks

The solvent adducts $[MoO_2Cl_2(L)_2]$ containing *N*,*N*-dialkylamide ligands exhibit very high initial activities in the epoxidation of *cis*-cyclooctene with tbhp under mild conditions (30–55 °C) and in the absence of cosolvents. These complexes are easy to prepare and are relatively stable to air and moisture. The turnover frequencies at 55 °C lie at the top end of the range (10–600 $mol\,mol_{Mo}^{-1}\,h^{-1}$) found for the same reaction under similar conditions with the use of $[MoO_2Cl_2(L')_n]$ complexes containing two monodentate ligands or one bidentate ligand, with most falling below 250 $mol\,mol_{Mo}^{-1}\,h^{-1}$. It must be noted that the catalytic epoxidation reactions with the $[MoO_2Cl_2(L)_2]$ complexes were very clean, giving the epoxide quantitatively within a few hours. Changing the nature of the substituents (H, methyl, ethyl, phenyl) on the carbonyl group and nitrogen atom of the *N*,*N*-dialkylamide does not lead to measurably different catalytic behaviour, and indeed very similar results are obtained by using the complexes with L = CH_3CN and thf, or even the precursor MoO_2Cl_2. The very high initial activities are offset by the decreased reaction rates in the second runs. Whereas the accumulation of *tert*-butyl alcohol coupled with the dilution of the reaction mixture in the second run could have some influence, the evidence suggests that the major cause is the formation of binuclear species with a structure similar to that determined for $[Mo_2O_4(\mu_2\text{-}O)Cl_2(dmf)_4]$, which was isolated from the reaction of $[MoO_2Cl_2(dmf)_2]$ with an excess amount of tbhp.

Experimental Section

Materials and Methods: Microanalyses for CHN were performed at the University of Aveiro. IR spectra were obtained as KBr pellets by using an FTIR Mattson-7000 infrared spectrophotometer. Raman spectra were recorded with a Bruker RFS100/S FT instrument (Nd:YAG laser, 1064 nm excitation, InGaAs detector). ^1H NMR spectra were acquired at room temperature by using a Bruker CXP 300 spectrometer and referenced to TMS. All preparations and manipulations were carried out by using standard Schlenk techniques under an atmosphere of N_2. Anhydrous dichloromethane and MoO_2Cl_2 were obtained from Aldrich and used as received. Hexane and diethyl ether were dried by standard procedures (Na/benzophenone ketyl), distilled, and kept under an atmosphere of N_2 over 4 Å molecular sieves. The complex $[MoO_2Cl_2(dmf)_2]$ (**1**) was synthesised as described previously by treatment of an aqueous

hydrochloric acid solution of MoO_3 with an excess amount of dmf[8a] and gave satisfactory elemental analyses, FTIR and NMR spectroscopic data. The tbhp (5.5 M in decane, ca. 5 wt.-% water) was used as received.

General Method for the Preparation of Complexes 2–5: A suspension of MoO_2Cl_2 (1.0 g, 5.0 mmol) in CH_2Cl_2 (30 mL) was treated with the ligand (2 equiv.). The solution was stirred for 2 h, filtered and evaporated to dryness in vacuo, and the resultant light-yellow solid was washed with diethyl ether and dried in vacuo.

$[MoO_2Cl_2(dma)_2]$ (2; dma = *N*,*N*-dimethylacetamide): Yield: 1.80 g, 96%. $C_8H_{18}Cl_2MoN_2O_4$ (373.09): calcd. C 25.75, H 4.85, N 7.5; found C 25.85, H 5.2, N 7.45. ^{1}H NMR (300 MHz, $CDCl_3$): δ = 2.42 [s, 6 H, $CH_3C(O)$], 3.14 [s, 12 H, $N(CH_3)_2$] ppm. IR (KBr): $\tilde{\nu}$ = 1608 (vs, ν_{CO}), 1509 (m, ν_{CN} of OC–N), 950 (s), 911 (vs, $\nu_{Mo=O}$) cm^{-1}. Raman: $\tilde{\nu}$ = 1505 (w), 947 (s), 909 (w) cm^{-1}.

$[MoO_2Cl_2(dmpa)_2]$ (3; dmpa = *N*,*N*-dimethylpropionamide): Yield: 1.73 g, 86%. $C_{10}H_{22}Cl_2MoN_2O_4$ (401.14): calcd. C 29.95, H 5.55, N 7.0; found C 30.15, H 5.95, N 6.95. ^{1}H NMR (300 MHz, $CDCl_3$): δ = 1.29 [t, 6 H, $CH_3CH_2C(O)$], 2.74 [q, 4 H, $CH_3CH_2C(O)$], 3.17 [s, 12 H, $N(CH_3)_2$] ppm. IR (KBr): $\tilde{\nu}$ = 1602 (vs, ν_{CO}), 1510 (m, ν_{CN} of OC–N), 950 (s), 911 (s, $\nu_{Mo=O}$) cm^{-1}. Raman: $\tilde{\nu}$ = 1514 (w), 946 (vs), 906 (w) cm^{-1}.

$[MoO_2Cl_2(def)]$ (4; def = *N*,*N*-diethylformamide): Yield: 1.85 g, 92%. $C_{10}H_{22}Cl_2MoN_2O_4$ (401.14): calcd. C 29.95, H 5.55, N 7.0; found C 30.2, H 5.9, N 6.95. ^{1}H NMR (300 MHz, $CDCl_3$): δ = 1.22–1.33 [m, 12 H, $N(CH_2CH_3)_2$], 3.42–3.54 [m, 8 H, $N(CH_2CH_3)_2$], 8.35 [s, 2 H, HC(O)] ppm. IR (KBr): $\tilde{\nu}$ = 1637 (vs, ν_{CO}), 945 (s), 908 (s, $\nu_{Mo=O}$) cm^{-1}. Raman: $\tilde{\nu}$ = 943 (vs), 915 (w) cm^{-1}.

$[MoO_2Cl_2(dpf)_2]$ (5; dpf = *N*,*N*-diphenylformamide): Yield: 2.7 g, 91%. $C_{26}H_{22}Cl_2MoN_2O_4$ (593.31): calcd. C 52.65, H 3.75, N 4.7; found C 52.45, H 3.55, N 5.1. ^{1}H NMR (300 MHz, $CDCl_3$): δ = 7.12–7.42 (m, 20 H, phenyl-H), 8.73 [s, 2 H, HC(O)] ppm. IR (KBr): $\tilde{\nu}$ = 1630 (vs), 1618 (vs, ν_{CO}), 950 (s), 910 (s, $\nu_{Mo=O}$) cm^{-1}. Raman: $\tilde{\nu}$ = 951 (s), 912 (w) cm^{-1}.

$[Mo_2O_4(\mu_2\text{-}O)Cl_2(dmf)_4]$ (6; dmf = *N*,*N*-dimethylformamide): A solution of $[MoO_2Cl_2(dmf)_2]$ (0.3 g, 0.87 mmol) in dmf (6 mL) was treated with tbhp (5.5 M in decane, 13 mmol), and the solution was stirred in an ice bath for 2 h. A mixture of hexane and diethyl ether was then added to initiate precipitation of a solid, and the mixture was left to age at –30 °C for 3 d. After complete precipitation, the solution was filtered off and the solid dried in vacuo. Yield: 0.19 g, 69%. $C_{12}H_{28}Cl_2Mo_2N_4O_9$ (635.16): calcd. C 22.7, H 4.45, N 8.8; found C 22.65, H 4.5, N 8.75. ^{1}H NMR (300 MHz, CD_3COCD_3): δ = 2.84 (s, 6 H, N-CH_3), 2.93 (s, 12 H, N-CH_3), 3.01 (s, 6 H, N-CH_3), 8.03 [s, 4 H, HC(O)] ppm. IR (KBr): $\tilde{\nu}$ = 1649 (vs, ν_{CO}), 948 (s), 903 (vs, $\nu_{Mo=O}$), 767 (vs, $\nu_{Mo-O-Mo}$) cm^{-1}. Raman: $\tilde{\nu}$ = 939 (vs), 902 (m, $\nu_{Mo=O}$) cm^{-1}.

Single-Crystal X-ray Diffraction: Details of the crystallographic data collection and structure refinement are summarised in Table 6. Single crystals of **6** suitable for X-ray analysis were obtained by slow evaporation of a solution of the complex in dmf. A single crystal was manually harvested from the crystallisation vial and mounted on a Hampton Research CryoLoop using Fomblin Y perfluoropolyether vacuum oil (Aldrich LVAC 25/6)[30] with the help of a Stemi 2000 stereomicroscope equipped with Carl Zeiss lenses. Data were collected at 100(2) K with a Bruker X8 Kappa APEX II CCD area-detector diffractometer (Mo-K_α graphite-monochromated radiation, λ = 0.7107 Å) controlled by the APEX2 software package,[31] and equipped with an Oxford Cryosystems Series 700 cryostream monitored remotely by using the software interface Cryopad.[32] Images were processed by using the software package SAINT+,[33] and data were corrected for absorption by the multiscan semiempirical method implemented in SADABS.[34] The structure was solved by using the Patterson synthesis algorithm implemented in SHELXS-97,[35] which allowed the immediate location of the crystallographically independent Mo^{VI} centre and the coordinated chlorido ligand. All remaining non-hydrogen atoms were directly located from difference Fourier maps calculated from successive full-matrix least-squares refinement cycles on F^2 by using SHELXL-97.[36] Non-hydrogen atoms were successfully refined by using anisotropic displacement parameters. Hydrogen atoms were located at their idealised positions by using appropriate *HFIX* instructions in SHELXL (*43* and *137* for the formamide and methyl groups of dmf, respectively) and included in subsequent refinement cycles in riding-motion approximation with isotropic thermal displacement parameters (U_{iso}) fixed at 1.2 or 1.5, respectively, times U_{eq} of the carbon atom to which they are attached. The last difference Fourier map synthesis showed the highest peak (0.871 e Å^{-3}) and deepest hole (–1.031 e Å^{-3}) located at 0.83 Å and 0.78 Å from Mo(1). Selected bond lengths and angles for the Mo^{VI} coordination environment are collected in Table 1. CCDC-654609 contains the supplementary crystallographic data for this paper. These data can be obtained free of charge from The Cambridge Crystallographic Data Centre via www.ccdc.cam.ac.uk/data_request/cif.

Table 6. Crystal and structure refinement data for $[Mo_2O_4(\mu_2\text{-}O)Cl_2(dmf)_4]$ (**6**).

Formula	$C_{12}H_{28}Cl_2Mo_2N_4O_9$
Formula weight	635.16
Crystal system	monoclinic
Space group	*C*2/*c*
a [Å]	12.6523(7)
b [Å]	13.3656(7)
c [Å]	13.1889(7)
β [°]	90.952(4)
Volume [Å^3]	2230.0(2)
Z	4
$D_{calcd.}$ [g cm^{-3}]	1.892
μ(Mo-K_α) [mm^{-1}]	1.414
Crystal size [mm]	0.18 × 0.16 × 0.08
Crystal type	colourless blocks
θ range	3.78 to 30.49
Index ranges	$-17 \le h \le 17$
	$-19 \le k \le 17$
	$-18 \le l \le 18$
Reflections collected	20032
Independent reflections	3364 (R_{int} = 0.0564)
Completeness to θ = 30.49°	99.2%
Final *R* indices [$I > 2\sigma(I)$][a,b]	R_1 = 0.0331
	wR_2 = 0.0709
Final *R* indices (all data)[a,b]	R_1 = 0.0497
	wR_2 = 0.0774
Weighting scheme[c]	*m* = 0.0362
	n = 1.6573
Largest diff. peak and hole	0.871 and –1.031 e Å^{-3}

[a] $R_1 = \Sigma||F_o| - |F_c||/\Sigma|F_o|$. [b] $wR_2 = \sqrt{\Sigma[w(F_o^2 - F_c^2)^2]/\Sigma[w(F_o^2)^2]}$. [c] $w = 1/[\sigma^2(F_o^2) + (mP)^2 + nP]$, where $P = (F_o^2 + 2F_c^2)/3$.

Catalysis: The liquid-phase catalytic epoxidations were carried out at atmospheric pressure in a reaction vessel equipped with a magnetic stirrer and immersed in a thermostatted oil bath. Typically, the microvessel was loaded with the complex (18 μmol), olefin (1.8 mmol) and oxidant (2.75 mmol, 5.5 M tbhp in decane or 70% aq. tbhp) without additional solvent (other than the decane present in the tbhp solution) or with ethanol, 1,2-dichloroethane (dce) or acetonitrile (2 mL). Different substrates were studied, namely, *cis*-cyclooctene, (*R*)-(+)-limonene, α-(+)-pinene and norbornene in the

presence of dce (2 mL). The course of the reaction was monitored by using a Varian 3800 GC equipped with a capillary column (DB-5, 30 m × 0.25 mm) and a flame ionisation detector. The products were identified by GC–MS (HP 5890 Series II GC and HP 5970 Series Mass Selective Detector) using He as the carrier gas. Undecane was used as the internal standard added after the reaction.

Kinetic Studies of Catalyst Formation: All kinetic measurements were carried by out using a large excess of tbhp (pseudo-first-order conditions). Typically, an appropriate small quantity of concentrated tbhp (5.5 M in decane) was added to a thermostatted UV quartz cell containing an appropriate amount of a solution of the metal complex in CH_3CN in order to obtain a total volume of 3 mL with final concentration of molybdenum compound equal to 3 to 4×10^{-4} M. The product formation was monitored against time by following absorbance changes at a specific wavelength in the range 300–500 nm by using a Varian Cary Bio50 UV/Vis spectrophotometer equipped with a thermostatted multiple cell holder.

Supporting Information (see also the footnote on the first page of this article): UV/Vis spectra for the reaction of **1** with tbhp at 25 °C; k_{obs} values for all complexes and reaction temperatures.

Acknowledgments

We are grateful to the Fundação para a Ciência e a Tecnologia (FCT), the Programa Operacional "Ciência e Inovação 2010" (POCI 2010), the Orçamento do Estado (OE) and the Fundo Europeu de Desenvolvimento Regional (FEDER) (Project POCI/QUI/56109/2004) for funding. B.M., P.N. and S.G. thank the FCT for grants. We are also grateful to the FCT for financial support towards the purchase of the single-crystal diffractometer.

[1] a) J. M. Tunney, J. McMaster, C. D. Garner, *Comprehensive Coordination Chemistry II* (Eds.: J. A. McCleverty, T. J. Meyer), Elsevier, Amsterdam, **2004**, vol. 8, pp. 459–477; b) J. H. Enemark, J. J. A. Cooney, J.-J. Wang, R. H. Holm, *Chem. Rev.* **2004**, *104*, 1175–1200; c) C. J. Whiteoak, G. J. P. Britovsek, V. C. Gibson, A. J. P. White, *Dalton Trans.* **2009**, 2337–2344; d) A. L. Bingham, J. E. Drake, M. B. Hursthouse, M. E. Light, R. Kumar, R. Ratnani, *Polyhedron* **2006**, *25*, 3238–3244; e) R. J. Butcher, B. R. Penfold, E. Sinn, *J. Chem. Soc., Dalton Trans.* **1979**, 668–675.

[2] a) F. J. Arnáiz, R. Aguado, J. M. Martinez de llarduya, *Polyhedron* **1994**, *13*, 3257–3259; b) F. J. Arnáiz, R. Aguado, M. R. Pedrosa, A. D. Cian, *Inorg. Chim. Acta* **2003**, *347*, 33–40; c) F. J. Arnáiz, R. Aguado, M. R. Pedrosa, J. Mahía, M. A. Maestro, *Polyhedron* **2002**, *21*, 1635–1642.

[3] a) F. E. Kühn, M. Groarke, É. Bencze, E. Herdtweck, A. Prazeres, A. M. Santos, M. J. Calhorda, C. C. Romão, I. S. Gonçalves, A. D. Lopes, M. Pillinger, *Chem. Eur. J.* **2002**, *8*, 2370–2383; b) F. E. Kühn, A. M. Santos, M. Abrantes, *Chem. Rev.* **2006**, *106*, 2455–2475; c) S. M. Bruno, B. Monteiro, M. S. Balula, C. Lourenço, A. A. Valente, M. Pillinger, P. Ribeiro-Claro, I. S. Gonçalves, *Molecules* **2006**, *11*, 298–308; d) S. M. Bruno, C. C. L. Pereira, M. S. Balula, M. Nolasco, A. A. Valente, A. Hazell, M. Pillinger, P. Ribeiro-Claro, I. S. Gonçalves, *J. Mol. Catal. A* **2007**, *261*, 79–87; e) G. Wang, G. Chen, R. L. Luck, Z. Wang, Z. Mu, D. G. Evans, X. Duan, *Inorg. Chim. Acta* **2004**, *357*, 3223–3229; f) A. Jimtaisong, R. L. Luck, *Inorg. Chem.* **2006**, *45*, 10391–10402; g) L. Feng, E. Urnezius, R. L. Luck, *J. Organomet. Chem.* **2008**, *693*, 1564–1571.

[4] a) M. L. Larson, F. W. Moore, *Inorg. Chem.* **1966**, *5*, 801–805; b) L. R. Florian, E. R. Corey, *Inorg. Chem.* **1968**, *7*, 722–725; c) J. E. Drake, M. B. Hursthouse, M. E. Light, R. Kumar, R. Ratnani, *J. Chem. Crystallogr.* **2007**, *37*, 421–427.

[5] C. D. Nunes, A. A. Valente, M. Pillinger, J. Rocha, I. S. Gonçalves, *Chem. Eur. J.* **2003**, *9*, 4380–4390.

[6] N. Manwani, M. C. Gupta, R. Ratnani, J. E. Drake, M. B. Hursthouse, M. E. Light, *Inorg. Chim. Acta* **2004**, *357*, 939–945.

[7] F. E. Kühn, E. Herdtweck, J. J. Haider, W. A. Herrmann, I. S. Gonçalves, A. D. Lopes, C. C. Romão, *J. Organomet. Chem.* **1999**, *583*, 3–10.

[8] a) F. J. Arnaiz, R. Aguado, J. Sanz-Aparicio, M. Martinez-Ripoll, *Polyhedron* **1994**, *13*, 2745–2749; b) F. J. Arnáiz, R. Aguado, M. R. Pedrosa, J. Mahía, M. A. Maestro, *Polyhedron* **2001**, *20*, 2781–2785; c) W. Levason, R. Ratnani, G. Reid, M. Webster, *Inorg. Chim. Acta* **2006**, *359*, 4627–4630.

[9] a) M. B. Hursthouse, W. Levason, R. Ratnani, G. Reid, *Polyhedron* **2004**, *23*, 1915–1921; b) M. F. Davis, W. Levason, R. Ratnani, G. Reid, T. Rose, M. Webster, *Eur. J. Inorg. Chem.* **2007**, 306–313.

[10] K. Dreisch, C. Andersson, M. Håkansson, S. Jagner, *J. Chem. Soc., Dalton Trans.* **1993**, 1045–1049.

[11] a) A. M. Al-Ajlouni, A. Günyar, M.-D. Zhou, P. N. W. Baxter, F. E. Kühn, *Eur. J. Inorg. Chem.* **2009**, 1019–1026; b) F. E. Kühn, A. D. Lopes, A. M. Santos, E. Herdtweck, J. J. Haider, C. C. Romão, A. G. Santos, *J. Mol. Catal. A* **2000**, *151*, 147–160; c) F. E. Kühn, A. M. Santos, A. D. Lopes, I. S. Gonçalves, E. Herdtweck, C. C. Romão, *J. Mol. Catal. A* **2000**, *164*, 25–38.

[12] a) M. D. Brown, M. B. Hursthouse, W. Levason, R. Ratnani, G. Reid, *Dalton Trans.* **2004**, 2487–2491; b) M. F. Davis, W. Levason, M. E. Light, R. Ratnani, G. Reid, K. Saraswat, M. Webster, *Eur. J. Inorg. Chem.* **2007**, 1903–1910.

[13] G. Barea, A. Lledos, F. Maseras, Y. Jean, *Inorg. Chem.* **1998**, *37*, 3321–3325.

[14] R. Sanz, R. Aguado, M. R. Pedrosa, F. J. Arnáiz, *Synthesis* **2002**, 856–858.

[15] K. Jeyakumar, D. K. Chand, *Appl. Organomet. Chem.* **2006**, *20*, 840–844.

[16] a) P. Chaumette, H. Mimoun, L. Saussine, J. Fischer, A. Mitschler, *J. Organomet. Chem.* **1983**, *250*, 291–310; b) B. Monteiro, S. S. Balula, S. Gago, C. Grosso, S. Figueiredo, A. D. Lopes, A. A. Valente, M. Pillinger, J. P. Lourenço, I. S. Gonçalves, *J. Mol. Catal. A* **2009**, *297*, 110–117.

[17] R. Sanz, J. Escribano, M. R. Pedrosa, R. Aguado, F. J. Arnáiz, *Adv. Synth. Catal.* **2007**, *349*, 713–718.

[18] R. J. Butcher, H. P. Gunz, R. G. A. R. Maclagan, H. K. J. Powell, C. J. Wilkins, *J. Chem. Soc., Dalton Trans.* **1975**, 1223–1227.

[19] W. E. Bull, S. K. Madan, J. E. Willis, *Inorg. Chem.* **1963**, *2*, 303–306.

[20] L. O. Atovmyan, Y. A. Sokolova, V. V. Tkachev, *Dokl. Akad. Nauk SSSR* **1970**, *195*, 1355–1356.

[21] a) F. H. Allen, *Acta Crystallogr., Sect. B: Struct. Sci.* **2002**, *58*, 380–388; b) F. H. Allen, W. D. S. Motherwell, *Acta Crystallogr., Sect. B: Struct. Sci.* **2002**, *58*, 407–422.

[22] M. V. Caparelli, B. Piggott, S. D. Thorpe, R. N. Sheppard, *Inorg. Chim. Acta* **1985**, *98*, L53–L55.

[23] J. A. Craig, E. W. Harlan, B. S. Snyder, M. A. Whitener, R. H. Holm, *Inorg. Chem.* **1989**, *28*, 2082–2091.

[24] F. J. Arnáiz, R. Aguado, M. R. Pedrosa, A. De Cian, J. Fischer, *Polyhedron* **2000**, *19*, 2141–2147.

[25] C. P. Rao, A. Sreedhara, P. V. Rao, M. B. Verghese, K. Rissanen, E. Kolehmainen, N. K. Lokanath, M. A. Sridhar, J. S. Prasad, *J. Chem. Soc., Dalton Trans.* **1998**, 2383–2393.

[26] A. Al-Ajlouni, A. A. Valente, C. D. Nunes, M. Pillinger, A. M. Santos, J. Zhao, C. C. Romão, I. S. Gonçalves, F. E. Kühn, *Eur. J. Inorg. Chem.* **2005**, 1716–1723.

[27] A. A. Valente, J. Moreira, A. D. Lopes, M. Pillinger, C. D. Nunes, C. C. Romão, F. E. Kühn, I. S. Gonçalves, *New J. Chem.* **2004**, *28*, 308–313.

[28] J. B. Lewis, G. W. Hedrick, *J. Org. Chem.* **1965**, *30*, 4271–4275.

[29] P. J. Kunkeler, J. C. van der Waal, J. Bremmer, B. J. Zuurdeeg, R. S. Downing, H. van Bekkum, *Catal. Lett.* **1998**, *53*, 135–138.
[30] T. Kottke, D. Stalke, *J. Appl. Crystallogr.* **1993**, *26*, 615–619.
[31] *APEX2, Data Collection Software*, version 2.1-RC13, Bruker AXS, Delft, The Netherlands, **2006**.
[32] *Cryopad, Remote Monitoring and Control*, version 1.451, Oxford Cryosystems, Oxford, UK, **2006**.
[33] *SAINT+, Data Integration Engine*, version 7.23a, Bruker AXS, Madison, WI, USA, **2005**.
[34] G. M. Sheldrick, *SADABS*, *Bruker/Siemens Area Detector Absorption Correction Program*, version 2.01, Bruker AXS, Madison, WI, USA, **1998**.
[35] G. M. Sheldrick, *SHELXS-97*, *Program for Crystal Structure Solution*, University of Göttingen, Göttingen, Germany, **1997**.
[36] G. M. Sheldrick, *SHELXL-97*, *Program for Crystal Structure Refinement*, University of Göttingen, Göttingen, Germany, **1997**.

Received: June 16, 2009
Published Online: September 10, 2009

